Eulerian Motion Magnification as an Imaging Biomarker for Acute Rheumatic Fever in Pediatric Echocardiography

Naila Suele Mascarenhas Silva[1], **Carlos Alberto Rodrigues**[1], **Airandes de Sousa Pinto**[2], **Bráulio Muzzi Ribeiro de Oliveira**[3], **Renata Fonseca Mendoza**[2], **Maria do Carmo Pereira Nunes**[4]

[1]Departamento de Ciências Exatas, UEFS, Feira de Santana, BA, Brasil

[2]Departamento de Saúde, UEFS, Feira de Santana, BA, Brasil

[3]Inst. de Previdência dos Servidores do Estado de MG (IPSEMG), Belo Horizonte, MG

[4]Faculdade de Medicina, UFMG, Belo Horizonte, MG, Brasil

nailasuely@ecomp.uefs.br, carod@uefs.br

Abstract. *In acute rheumatic fever (ARF), valvular involvement is inflammatory and precedes the structural remodeling of chronic disease; as a result, descriptors built on leaflet geometry or kinematics often fail to separate ARF from controls in this early window. We ask whether the global cardiac motion of the exam, amplified by Eulerian Video Magnification (EVM), carries a signature of ARF in two-dimensional pediatric echocardiography. For each study, a temporal band-pass filter isolates the heartbeat-frequency component of intensity variation, and the energy of that motion is summarized into compact descriptors. Across 73 examinations (17 ARF, 56 controls), motion-energy descriptors were higher in ARF ($p < 0.01$; Cohen's d up to 0.80) and, under leave-one-out cross-validation, separated the groups with an area under the ROC curve of 0.69 (95% CI 0.53–0.83; permutation $p = 0.022$). Direct leaflet kinematic descriptors did not separate the groups (AUC 0.42) under the same protocol. These preliminary results place amplified global motion as an objective, low-cost candidate marker for ARF screening in resource-limited settings, and they motivate validation on larger, multi-center cohorts.*

1. Introduction

Rheumatic heart disease (RHD) remains the leading cause of acquired heart disease among children and young adults in low-income regions, accounting for more than 300,000 deaths each year and a burden that falls disproportionately on socioeconomically vulnerable populations [Watkins et al. 2017, Zühlke et al. 2015]. Its origin is acute rheumatic fever (ARF), a delayed autoimmune sequela of group A *Streptococcus* pharyngitis, in which cross-reactive antibodies attack the valvular endocardium and trigger valvulitis [Passos et al. 2021]. Early recognition matters because it enables secondary prophylaxis with benzathine penicillin, a low-cost intervention that prevents recurrences and halts valvular progression [Reményi et al. 2012].

Two-dimensional echocardiography is the reference modality for this recognition, and the World Heart Federation guidelines define morphological and regurgitation criteria, with particular weight on the anterior mitral leaflet [Reményi et al. 2012,

Gewitz et al. 2015]. Two factors, however, limit echocardiography as a large-scale screening tool. The first is access, since the exam is operator-dependent and requires a cardiologist for interpretation, a resource scarce precisely in endemic regions [Nunes et al. 2016]. The second is intrinsic to the acute phase. Unlike chronic rheumatic stenosis, where decades of remodeling produce measurable thickening, calcification, and restricted mobility, acute involvement is inflammatory and has not yet consolidated into clear structural change [Passos et al. 2021]. The characteristic lesions, small verrucous nodules along the coaptation lines, are millimetric and transient, and the valve can look morphologically normal even with pathological regurgitation [Passos et al. 2021, Gewitz et al. 2015].

This subtlety explains why computational descriptors based on leaflet *geometry* (thickness, area) or *direct kinematics* (velocity, deformation) tend to discriminate poorly in ARF, since the relevant signal is spread diffusely across the exam and not localized in one structure. Capturing the *functional* manifestations of acute inflammation therefore calls for a different kind of descriptor.

We start from the hypothesis that, even when the isolated leaflet looks preserved, acute carditis alters the *global dynamics* of the exam, through regurgitation and a more energetic tissue-motion pattern, in a way that escapes visual inspection. To expose and quantify this signal we adopt Eulerian Video Magnification (EVM), a video-processing technique that amplifies subtle temporal variations without explicitly tracking structures [Wu et al. 2012]. Conceived to make visible the blood flow in a face and other tiny movements, EVM has since been carried over to non-invasive vital-sign monitoring and, more recently, to heart-failure surveillance [Abnousi et al. 2019]. Its application to rheumatic disease, and in particular to the acute phase, is not reported in the literature we surveyed.

The contributions of this work are: (i) to **formulate** an EVM-based pipeline for characterizing ARF in 2D echocardiography that requires no segmentation and no structure tracking; (ii) to **propose** compact *motion-energy* descriptors in the heartbeat band, defined as a quantity proportional to the squared amplitude of local motion; and (iii) to **evaluate**, with leakage-free cross-validation and a permutation test, how well these descriptors separate ARF from controls, contrasting them with direct leaflet kinematic descriptors on the same cohort.

2. Related Work

Positioning this work calls for three lines of research: computational screening for rheumatic disease, motion analysis in echocardiography, and video motion magnification.

2.1. Computational screening for rheumatic disease

The shortage of specialists has driven screening strategies based on portable equipment and remote interpretation. The PROVAR program showed that Brazilian schoolchildren can be screened with handheld devices operated by non-experts and read remotely by cardiologists [Nunes et al. 2016], and related studies confirmed the accuracy of lay-operator screening [Ploutz et al. 2016]. On this basis, deep-learning methods began to automate interpretation. Martins et al. proposed a 3D video model for the automatic diagnosis of RHD from exams acquired by non-experts [Martins et al. 2021], and Brown et al. compared classical and deep models for mitral regurgitation analysis, showing the value of interpretable descriptors [Brown et al. 2024]. More recent work extends automated screening

to other modalities, such as AI-enhanced electrocardiography [Bhorat et al. 2026], and recent reviews survey the expanding role of artificial intelligence in pediatric echocardiography [Wang et al. 2025] and in echocardiographic RHD screening with portable, non-expert-operated protocols [Williamson et al. 2024]. These approaches, however, target *established* RHD or regurgitation and depend on large annotated datasets; discrimination of the *acute* phase, with its subtle signature, remains little explored.

2.2. Motion analysis in echocardiography

Quantifying cardiac motion has long centered on *speckle* tracking, which estimates myocardial deformation (*strain*) by following texture patterns [Leitman et al. 2004], now standardized by international consensus [Voigt et al. 2015]. More recently, video-based deep models such as EchoNet-Dynamic reached reference performance in ejection-fraction estimation by integrating information across cardiac cycles [Ouyang et al. 2020], and video foundation models have since scaled this idea to large unlabeled echocardiogram datasets [Zhang et al. 2025, Kim et al. 2025]. All of these methods model the displacement of *specific structures* such as the myocardium, the leaflet, or the ventricle. Eulerian magnification takes the opposite stance and tracks no structure at all, amplifying the temporal signal of the whole scene, which makes it sensitive to *diffuse* motion that point tracking may discard as noise.

2.3. Video motion magnification

Eulerian video magnification was introduced by Wu et al. [Wu et al. 2012], who combined spatial pyramid decomposition with temporal filtering to amplify subtle variations in color and motion, recovering, for instance, the heart rate from imperceptible changes in skin tone. The multiscale decomposition traces back to the Laplacian pyramid of Burt and Adelson [Burt and Adelson 1983]. Wadhwa et al. recast the approach in the *phase* domain, more robust to noise and capable of larger amplification [Wadhwa et al. 2013], and later accelerated it with the efficient Riesz pyramid [Wadhwa et al. 2014]. Learning-based variants reduced amplification artifacts [Oh et al. 2018]. In the clinical domain, EVM has been applied to non-invasive vital-sign monitoring and to remote heart-failure surveillance [Abnousi et al. 2019] but, to the extent of the literature we surveyed, not to echocardiography of rheumatic disease.

These lines leave a gap that this work addresses. Eulerian motion magnification, a technique that captures diffuse dynamics without segmentation, has not been applied to the separation of acute ARF in low-cost 2D echocardiography.

3. Materials and Methods

Figure 1 summarizes the proposed pipeline, from the input video to the motion-energy descriptors.

3.1. Dataset

We analyzed two-dimensional pediatric echocardiograms from patients with ARF diagnosed according to the revised Jones criteria [Gewitz et al. 2015] and validated by a panel of specialists, together with controls. After excluding exams with acquisition failure or with failure to locate the structure of interest, the final analysis comprised 73 exams (17 ARF and 56 controls).

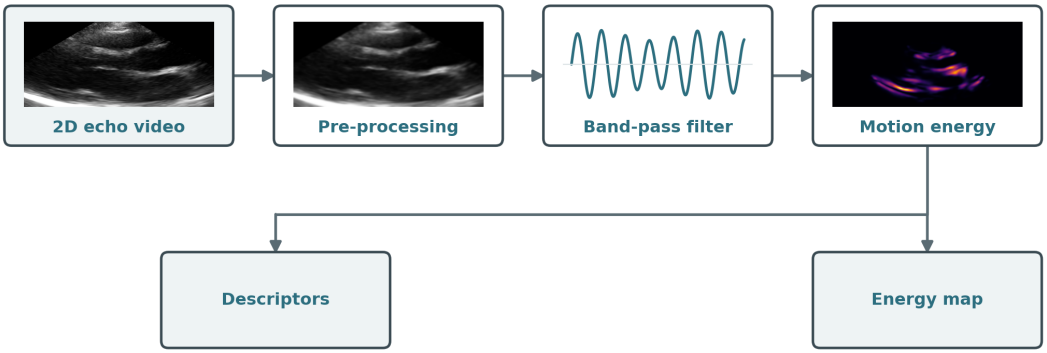


Figure 1. Proposed pipeline. The 2D echo video is pre-processed (grayscale conversion, downscaling, and smoothing) and passed through a temporal band-pass filter in the heartbeat band (1–3 Hz); the motion energy $P = B^2$ is then summarized into compact descriptors (mean energy, 95th percentile, and temporal variability) and into a spatial energy map. No step requires segmentation or structure tracking.

3.2. Eulerian Motion Magnification

The Eulerian approach [Wu et al. 2012] avoids computing the velocity field explicitly. Instead of tracking pixel displacement (the Lagrangian view), it analyzes the temporal variation of intensity at *fixed positions*. For a small displacement, an intensity change at a point approximates, to first order, the local motion; amplifying that change within a frequency band of interest therefore amplifies the associated motion. Spatial pyramid decomposition [Burt and Adelson 1983] and temporal filtering are the two pillars of the method; phase-based formulations add robustness to noise [Wadhwa et al. 2013]. Here we use the linear formulation, which is sufficient for the intended quantification and computationally light.

3.3. Processing pipeline

Each video was converted to grayscale and resized to 320×180 pixels, which lowers the computational cost and attenuates the *speckle* noise typical of ultrasound; a spatial Gaussian smoothing ($\sigma = 2$ pixels) preceded the temporal filtering. The first 100 frames of each exam were used. At each pixel along time we applied a second-order Butterworth band-pass filter [Oppenheim and Schafer 1999] in the 1–3 Hz range, matching the heart rate expected for this age group (60–180 bpm), in zero-phase mode (*filtfilt*). Writing $I(x, y, t)$ for the intensity at pixel (x, y) and time t, the filtered signal is

$$B(x, y, t) = \big(h_{[f_1, f_2]} * I(x, y, \cdot)\big)(t) \tag{1}$$

where $h_{[f_1,f_2]}$ is the impulse response of the filter with band $[f_1, f_2] = [1, 3]$ Hz. This filtering isolates the motion component locked to the heartbeat.

One distinction matters for reproducibility. Magnification proper, $I'(x, y, t) = I(x, y, t) + \alpha\, B(x, y, t)$ with gain α, serves only *visualization*, reconstructing a video in which subtle movements become perceptible to an observer. The quantitative descriptors

analyzed in this work were computed directly from the band signal B, without amplification. The result therefore does not depend on the choice of α, which removes one hyperparameter from the measurement procedure.

3.4. Motion-energy descriptors

We define the *motion energy* as the squared amplitude of the band, $P(x, y, t) = B(x, y, t)^2$, a quantity that grows with the strength of local motion in the heartbeat band. From it we derive, per exam, aggregate descriptors: the mean energy $\overline{P}$, its temporal dispersion σ_P, and the 95th percentile of the energy distribution P_{95}, which captures the strongest motion events. We also compute the spatial *energy map* $M(x, y) = \frac{1}{T}\sum_t P(x, y, t)$, which shows where motion concentrates over the exam and grounds the visual comparison between groups.

3.5. Statistical analysis

Group comparison used the Mann–Whitney U test, suited to non-normal distributions and unbalanced samples, with a significance level of $p < 0.05$ and effect size by Cohen's d. Discriminative ability was assessed with a logistic regression classifier over the energy descriptors, under leave-one-out cross-validation, a protocol recommended for small samples because it reduces the bias of the estimate. To avoid information leakage, descriptor standardization and classifier fitting were re-estimated within each fold, using the training exams only. We report the area under the ROC curve (AUC), with a 95% confidence interval by bootstrap, and the sensitivity and specificity at the maximum Youden index. A permutation test with shuffled labels, re-estimating the whole pipeline at each repetition, confirmed the significance of the AUC by estimating the performance distribution under the null hypothesis of no association.

3.6. Leaflet kinematic baseline

To isolate the contribution of the proposed descriptors, we compared them against a structural baseline based on the direct kinematics of the anterior mitral leaflet on the same cohort. From the leaflet position over the cardiac cycle we derived a set of kinematic descriptors: the tip and base excursions, the tip-to-base mobility ratio, the angular amplitude and the maximum angular velocity of the leaflet, and the mean and variance of its curvature. These descriptors were submitted to the *same* leakage-free leave-one-out protocol, logistic classifier, and permutation test used for the motion-energy descriptors, so that the comparison reflects only the choice of descriptor and not the evaluation procedure.

4. Results

4.1. Motion-energy descriptors

The motion-energy descriptors were consistently higher in the ARF group (Table 1). Mean energy ($p = 0.008$; $d = 0.74$), the 95th percentile ($p = 0.006$; $d = 0.76$), and temporal variability ($p = 0.011$; $d = 0.80$) differed between groups with large effect sizes by conventional thresholds. The distribution of the descriptors (Figure 3) shows an upward shift of the ARF values, with partial overlap between groups, consistent with the subtle nature of the phenomenon.

The group-averaged motion-energy map (Figure 2) illustrates the finding. The ARF group shows stronger and more spatially spread motion than controls, a pattern consistent with a diffuse dynamics associated with acute carditis.

Table 1. Motion-energy descriptors by group. Values are medians; p-value by the Mann–Whitney U test; Cohen's d as effect size.

Descriptor	ARF	Control	p	d
Mean energy $\overline{P}$	122.0	80.7	0.008	0.74
Energy (P95) P_{95}	614.5	397.2	0.006	0.76
Temporal variability σ_P	551.7	405.6	0.011	0.80

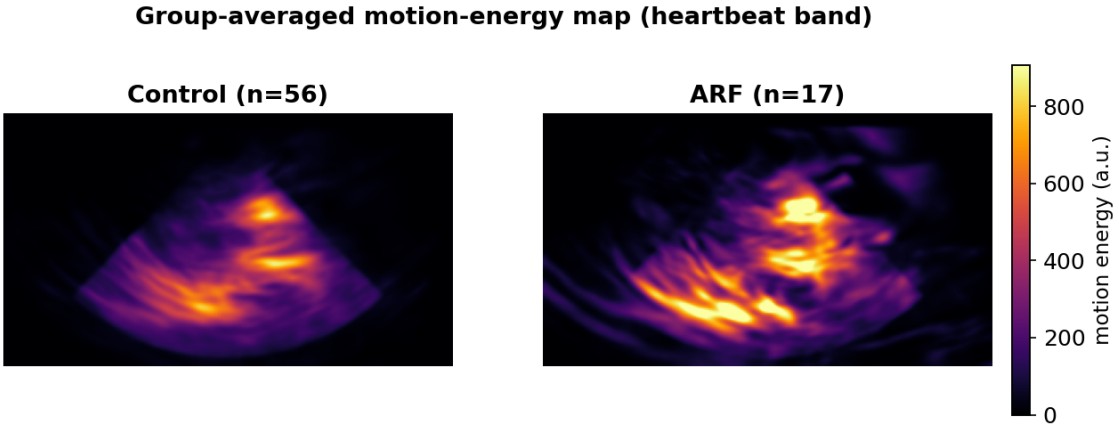


Figure 2. Group-averaged motion-energy map in the heartbeat band. On the right, ARF shows stronger and more diffuse energy than controls (left). The color scale is shared across panels.

4.2. Discriminative ability

Under leave-one-out cross-validation, a logistic classifier combining the energy descriptors separated ARF from controls with an AUC of 0.69 (95% CI: 0.53–0.83), with sensitivity 0.59 and specificity 0.71 at the maximum Youden index (Figure 4). The entire decision chain (descriptor standardization and classifier fitting) was re-estimated *within* each cross-validation fold, so that no test exam influenced the normalization or the model coefficients; the operating point derived from the Youden index is therefore descriptive and is not a post-hoc selection on the same data. The permutation test, with shuffled labels and the pipeline re-estimated at each repetition, confirmed that performance exceeds chance ($p = 0.022$), whose null distribution centers around 0.5.

The same validation protocol applied to direct leaflet kinematic descriptors (excursion, tip-to-base mobility ratio, angular velocity, and curvature) did not separate the groups, yielding an AUC of 0.42 (95% CI: 0.25–0.59), consistent with chance. The contrast between global motion energy (0.69) and leaflet kinematics (0.42) on the same cohort supports the central hypothesis that, in this acute window, the discriminative signal resides in the global dynamics of the exam rather than in one isolated structure.

5. Discussion

The main finding is that the energy of amplified global motion separates ARF from controls, whereas descriptors of the isolated leaflet, on the same cohort, do not. The signature of the acute phase therefore appears to lie in a *diffuse* manifestation of inflammation, while the geometry and kinematics of a specific structure remain preserved at this stage

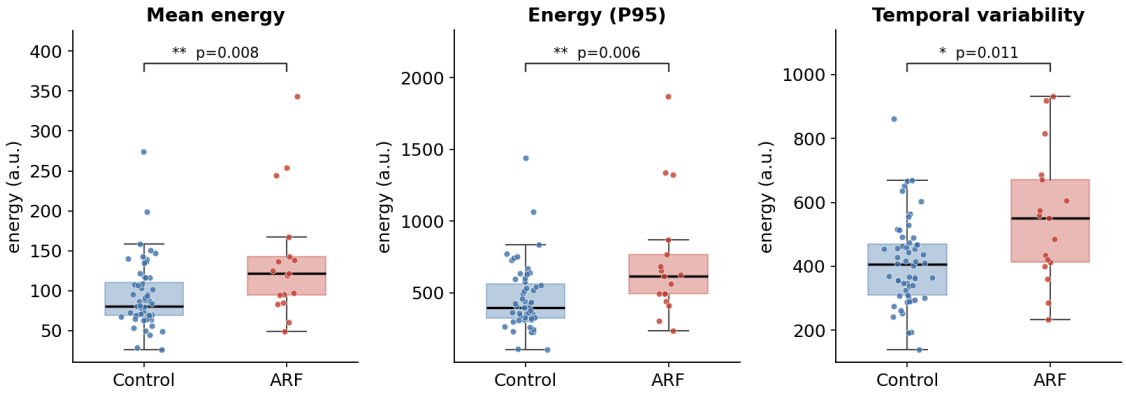


Figure 3. Distribution of the three motion-energy descriptors by group, with individual exams overlaid. The brackets mark statistical significance (Mann–Whitney U test).

[Passos et al. 2021]. EVM plausibly captures the joint dynamics of the exam, including the mitral regurgitation jet and the more energetic tissue-motion pattern associated with carditis, which point tracking of structures tends to discard. In the acute phase, valvulitis frequently produces mitral regurgitation even when leaflet morphology looks normal [Gewitz et al. 2015]; the regurgitant jet and the reactive myocardial motion add movement to the scene that the motion-energy descriptors capture as a whole. This reading is consistent with the pathophysiology, in which function changes before structure consolidates [Passos et al. 2021, Gewitz et al. 2015], and with the magnification literature, which shows that EVM reveals sub-perceptual motion absent from a direct structural analysis [Wu et al. 2012, Wadhwa et al. 2013].

From a screening standpoint, the approach is attractive for three reasons. First, it *requires no segmentation or tracking*, steps that demand annotation and trained models [Martins et al. 2021, Ouyang et al. 2020] and that break down under the low image quality typical of non-expert acquisitions [Nunes et al. 2016, Ploutz et al. 2016]. Second, it is *computationally light*, with temporal filtering of linear complexity [Oppenheim and Schafer 1999], compatible with real-time formulations [Wadhwa et al. 2014]. Third, it produces an *interpretable map* (Figure 2) that supports clinical trust by making explicit where motion concentrates.

The work has limitations that bound its conclusions. The cohort is small, unbalanced, and single-center, which widens the uncertainty, reflected in the broad confidence interval of the AUC, and rules out claims of equivalence or generalization. With 17 cases in the smaller group, the study is exploratory and hypothesis-generating. Motion energy is a *global* descriptor and, as such, is also sensitive to acquisition factors such as gain, depth, and acoustic window. Because acquisition parameters were not controlled prospectively across groups, we cannot rule out that part of the signal reflects systematic capture differences rather than carditis; this is the main threat to the internal validity of the finding. Confirming that the signal reflects the disease, and not the acquisition or patient discomfort, calls for a standardized capture protocol and, ideally, a fixed region of interest over the valve rather than the whole frame. For use as screening, moreover, the goal is to miss no cases, so the operating point should favor sensitivity; the Youden index balances the two errors and is not the ideal criterion here, and the sensitivity of

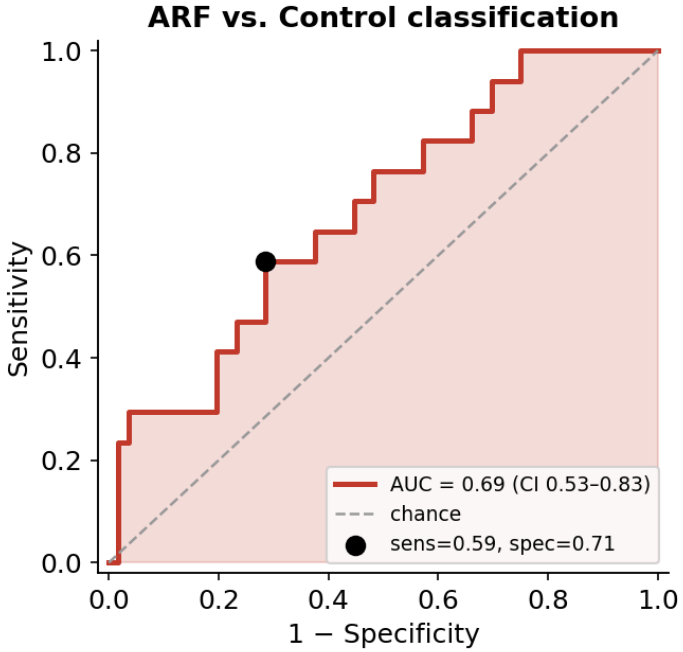


Figure 4. ROC curve for ARF *vs.* control classification using the motion-energy descriptors, under leave-one-out validation. The highlighted point is the maximum Youden index.

0.59 reported at that point is only descriptive. A screening-oriented model should instead fix a high target sensitivity (for example, ≥ 0.90) and report the resulting specificity. Finally, the validation is one of internal consistency, without an external reference standard (expert measurement or phantom), so the reported performance should be read as evidence of feasibility rather than established diagnostic accuracy. As work in progress, we plan to enlarge and diversify the cohort, to analyze the energy map regionally so as to localize the contribution of regurgitation, to compare with phase-based formulations [Wadhwa et al. 2013, Wadhwa et al. 2014], and to combine these descriptors with complementary ones.

6. Conclusion

This work studied Eulerian motion magnification as an imaging biomarker for acute rheumatic fever in two-dimensional pediatric echocardiography. The motion-energy descriptors in the heartbeat band were higher in ARF and separated the groups with an AUC of 0.69 under leakage-free cross-validation, a performance confirmed by a permutation test, in a regime where direct leaflet kinematic descriptors, under the same protocol, did not separate the groups (AUC 0.42). The result, still preliminary, indicates that amplified global motion captures a functional signal that escapes structural analysis, and points to EVM as a low-cost direction for ARF screening in resource-limited settings. Future work includes validation on larger, multi-center cohorts and comparison with reference measurements.

References

Abnousi, F., Kang, G., Giacomini, J., Yeung, A., Zarafshar, S., Vesom, N., Ashley, E., Harrington, R., and Yong, C. (2019). A novel noninvasive method for remote heart

failure monitoring: the eulerian video magnification applications in heart failure study (amplify). *npj Digital Medicine*, 2(1):80.

Bhorat, R., Harmon, D. M., Liu, K., Dugan, J., Ngo, C., Friedman, P. A., Bagula, H., Ntsekhe, M., and Attia, Z. I. (2026). Artificial intelligence-enhanced electrocardiogram for the detection of rheumatic heart disease. *European Heart Journal – Digital Health*, 7(4):ztag056.

Brown, K., Roshanitabrizi, P., Rwebembera, J., et al. (2024). Using artificial intelligence for rheumatic heart disease detection by echocardiography: focus on mitral regurgitation. *Journal of the American Heart Association*, 13(2):e031257.

Burt, P. J. and Adelson, E. H. (1983). The laplacian pyramid as a compact image code. *IEEE Transactions on Communications*, 31(4):532–540.

Gewitz, M. H., Baltimore, R. S., Tani, L. Y., et al. (2015). Revision of the jones criteria for the diagnosis of acute rheumatic fever in the era of doppler echocardiography: a scientific statement from the american heart association. *Circulation*, 131(20):1806–1818.

Kim, S., Jin, P., Song, S., Chen, C., Li, Y., Ren, H., Li, X., Liu, T., and Li, Q. (2025). EchoFM: Foundation model for generalizable echocardiogram analysis. *IEEE Transactions on Medical Imaging*.

Leitman, M., Lysyansky, P., Sidenko, S., et al. (2004). Two-dimensional strain—a novel software for real-time quantitative echocardiographic assessment of myocardial function. *Journal of the American Society of Echocardiography*, 17(10):1021–1029.

Martins, J. F. B. S., Nascimento, E. R., Nascimento, B. R., et al. (2021). Towards automatic diagnosis of rheumatic heart disease on echocardiographic exams through video-based deep learning. *Journal of the American Medical Informatics Association*, 28(9):1834–1842.

Nunes, M. C. P., Sable, C., Nascimento, B. R., et al. (2016). Echocardiographic prevalence of rheumatic heart disease in brazilian schoolchildren: data from the provar study. *International Journal of Cardiology*, 219:439–445.

Oh, T.-H., Jaroensri, R., Kim, C., Elgharib, M., Durand, F., Freeman, W. T., and Matusik, W. (2018). Learning-based video motion magnification. In *Proceedings of the European Conference on Computer Vision (ECCV)*, pages 633–648.

Oppenheim, A. V. and Schafer, R. W. (1999). *Discrete-Time Signal Processing*. Prentice Hall, 2 edition.

Ouyang, D., He, B., Ghorbani, A., et al. (2020). Video-based ai for beat-to-beat assessment of cardiac function. *Nature*, 580(7802):252–256.

Passos, L. S. A., Nunes, M. C. P., and Aikawa, E. (2021). Rheumatic heart valve disease pathophysiology and underlying mechanisms. *Frontiers in Cardiovascular Medicine*, 7:612716.

Ploutz, M., Lu, J. C., Scheel, J., et al. (2016). Handheld echocardiographic screening for rheumatic heart disease by non-experts. *Heart*, 102(1):35–39.

Reményi, B., Wilson, N., Steer, A., et al. (2012). World heart federation criteria for echocardiographic diagnosis of rheumatic heart disease—an evidence-based guideline. *Nature Reviews Cardiology*, 9(5):297–309.

Voigt, J.-U., Pedrizzetti, G., Lysyansky, P., et al. (2015). Definitions for a common standard for 2d speckle tracking echocardiography: consensus document of the eacvi/ase/industry task force. *European Heart Journal – Cardiovascular Imaging*, 16(1):1–11.

Wadhwa, N., Rubinstein, M., Durand, F., and Freeman, W. T. (2013). Phase-based video motion processing. *ACM Transactions on Graphics (TOG)*, 32(4):1–10.

Wadhwa, N., Rubinstein, M., Durand, F., and Freeman, W. T. (2014). Riesz pyramids for fast phase-based video magnification. In *IEEE International Conference on Computational Photography (ICCP)*, pages 1–10. IEEE.

Wang, A., Doan, T. T., Reddy, C., and Jone, P.-N. (2025). Artificial intelligence in fetal and pediatric echocardiography. *Children*, 12(1):14.

Watkins, D. A., Johnson, C. O., Colquhoun, S. M., et al. (2017). Global, regional, and national burden of rheumatic heart disease, 1990–2015. *New England Journal of Medicine*, 377(8):713–722.

Williamson, J., Reményi, B., Francis, J., Morris, P., and Whalley, G. (2024). Echocardiographic screening for rheumatic heart disease: a brief history and implications for the future. *Heart, Lung and Circulation*, 33(7):943–950.

Wu, H.-Y., Rubinstein, M., Shih, E., Guttag, J., Durand, F., and Freeman, W. (2012). Eulerian video magnification for revealing subtle changes in the world. *ACM Transactions on Graphics (TOG)*, 31(4):1–8.

Zhang, Z., Wu, Q., Ding, S., Wang, X., and Ye, J. (2025). Echo-vision-fm: a pre-training and fine-tuning framework for echocardiogram video vision foundation model. *Nature Communications*, 16.

Zühlke, L., Engel, M. E., Karthikeyan, G., et al. (2015). Characteristics, complications, and gaps in evidence-based interventions in rheumatic heart disease: the global rheumatic heart disease registry (the remedy study). *European Heart Journal*, 36(18):1115–1122.